Dynamics and Control of 6-DOF Shaking Table with Bell Crank Structure

Duek-Jae Jeon*, Sung-Ho Park, Young-Jin Park, Youn-Sik Park,
Hyoung-Eui Kim and Jong-Won Park

* Center for Noise and Vibration Control, Dept. of Mech. Eng., KAIST, Daejeon, Korea
(Tel : +82-42-869-3060; E-mail: jdj0420@kaist.ac.kr)

Abstract: This paper describes the kinematics, dynamics and control of a 6-DOF shaking table with a bell crank structure, which converts the direction of reciprocating movements. In this shaking table, the bell crank mechanism is used to reduce the amount of space needed to install the shaking table and create horizontal displacement of the platform. In kinematics, joint design is performed using Grübler's formula. The inverse kinematics of the shaking table is discussed. The derivation of the Jacobian matrix is presented to evaluate singularity conditions. Considering the maximum stroke of the hydraulic actuator, collision between links and singularity, workspace is computed. In dynamics, computations are based on the Newton-Euler formulation. To derive parallel algorithms, each of the contact forces is decomposed into one acting in the direction of the leg and the other acting in the plane orthogonal to the direction of the leg. Applying the Newton-Euler approach, the solution of inverse dynamics is almost completely parallel. Only one of the steps – the application of the Newton-Euler equations to the platform – must be performed on one single processor. Finally, the efficient control scheme is proposed for the tracking control of the motion platform.

Keywords: Shaking Table, Bell Crank, Jacobian Matrix, Newton-Euler, Parallel Algorithm, Parallel Manipulator

1. INTRODUCTION

Many products and packages undergo vibration in real world environments. In transportation environment, they can suffer vibration via truck or rail. In operating environment, examples include electronics in vehicles, construction equipment and aircraft. Serious damage of many types of products is expected on this condition. Many products have to survive vibration in their daily working life regardless of any environments. Vibration testing, in brief, is the shaking or shocking of a component or assembly to see how it will stand up to real conditions. Its ability to survive in real world can be determined through vibration testing. The procedure for vibration testing is used in applications ranging from circuit boards and aircraft to vehicle and household appliances.

The vibration testing system or shaking table is a type of parallel manipulator. Typically a parallel manipulator consists of a moving platform connected by several legs to a fixed platform, usually called a base. The paradigm of parallel manipulators is the Gough-Stewart platform, which has 6 DOF. In recent years, parallel manipulators have drawn much attention of researchers and engineers in the area of robotics because they are known to provide better accuracy, rigidity, load-to-weight ratio and load distribution than serial manipulators [1]. It has been many research works about practical design to enlarge small workspace and low dexterity of parallel manipulators. However, most papers have dealt with its kinematic problems than the dynamic modeling and control.

This paper describes the kinematics, dynamics and control of 6-DOF shaking table with a bell crank structure. In kinematics, joint design is performed using Grübler's formula. The solution of inverse kinematics is obtained [3] and [6]. The Jacobian matrix is derived and used to evaluate singularity conditions [4]. Considering maximum stroke of the hydraulic actuator, collision between links and singularity, workspace is computed [5] and [7]-[8]. In dynamics, Newton-Euler method is introduced for dynamic formulation [2]. The parallel algorithm arises from a judicious choice of the coordinate frames attached to each of the legs, which allows for the exploitation of the parallel nature of the mechanism itself. For the tracking control of the platform, the efficient control algorithm is proposed.

This paper is organized as follows. In Section 2, kinematic problems such as joint design, inverse kinematics, Jacobian matrix and workspace are analyzed. In Section 3, using kinematic properties, dynamic equation is derived. We show that a parallel algorithm can be applied to the shaking table system. In Section 4, we propose a control algorithm for the tracking control. In Section 5, concluding remarks are followed.

2. KINEMATICS

2.1 Bell crank mechanism

The bell crank mechanism is used to convert the direction of reciprocating movement. In this shaking table, a bell crank structure is used to reduce the amount of space needed to install the shaking table and create horizontal displacement of the platform. The 6-DOF shaking table with a bell crank structure is shown in Fig. 1.

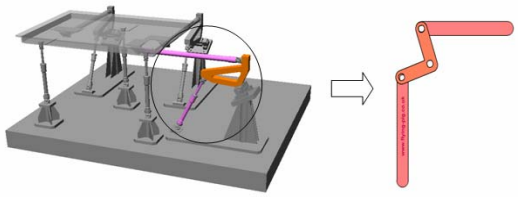

Fig. 1 The 6-DOF shaking table with a bell crank structure.

2.2 Joint design

In general, the number of degrees of freedom of a closed loop mechanism is not readily obvious. The total number of freedoms can be computed with Grübler's formula, expressed as

$$F = 6(l - j - 1) + f \,. \tag{1}$$

where F is the total number of degrees of freedom in the mechanism, l is the number of links including the base, j is the

total number of joints and *f* is the total number of degrees of freedom associated with joints.

This shaking table system has two types of hydraulic actuators. One is a straight actuator which is a general type. The other is a bell crank actuator which has a triangular bell crank structure. These two types of hydraulic actuators are shown in Fig. 2.

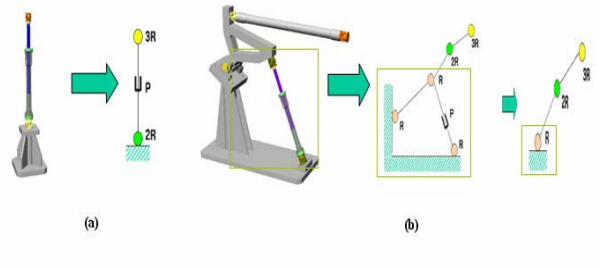

Fig. 2 Two types of hydraulic actuators in the shaking table.

The mechanism analyzed in this shaking table has 6 actuated prismatic (P) joints, revolute (R) joints, universal (2R) joints and spherical (3R) joints. In Fig. 2(a), the straight actuator consists of 3 (1 spherical, 1 prismatic and 1 universal) joints. In Fig. 2(b), the bell crank actuator consists of 6 (1 spherical, 1 prismatic, 1 universal and 3 revolute) joints. In case of a bell crank actuator, to analyze the degrees of freedom in the mechanism it is transformed into the equivalent link structure as shown in Fig. 2(b). Using Grübler's formula, we verify that the total number of freedoms is six, computed as

$$F = 6(14\text{-}18\text{-}1) + 36 = 6. \tag{2}$$

2.3 Inverse kinematics

The inverse kinematics can be described as: given the position and orientation of the moving platform, calculate the displacements of the actuating devices which can be used to attain this given position and orientation. To solve inverse kinematics, first it is necessary to establish a set of coordinate frames. The reference frame $A(O, x_A, y_A, z_A)$ is fixed to the base and the coordinate frame $B(P, x_B, y_B, z_B)$ is attached to the platform. Let ${}^{A}P$ and ${}^{A}_{B}R$ position and rotation of the moving frame B with respect to the base coordinate frame A. ${}^{A}_{B}R$ is a 3×3 matrix and ${}^{A}P$ is a 3×1 vector, which can be expressed as

$$\begin{aligned} {}^{A}_{B}R(\alpha,\beta,\gamma) &= R(\gamma)R(\beta)R(\alpha) \\ &= \begin{pmatrix} c\gamma c\beta & c\gamma s\beta s\alpha - s\gamma c\alpha & c\gamma s\beta c\alpha + s\gamma s\alpha \\ s\gamma c\beta & s\gamma s\beta s\alpha + c\gamma c\alpha & s\gamma s\beta c\alpha - c\gamma s\alpha \\ -s\beta & c\beta s\alpha & c\beta c\alpha \end{pmatrix} \\ {}^{A}P &= P_x x_A + P_y y_A + P_z z_A. \end{aligned} \tag{3}$$

In case of the straight actuator as shown in Fig. 3, using homogeneous transformation, we can write

$${}^{A}b_i = {}^{A}P + {}^{A}_{B}R\,{}^{B}b_i \quad i = 1,2,3. \tag{4}$$

where the left superscript indicates the reference frame in which a vector is expressed.

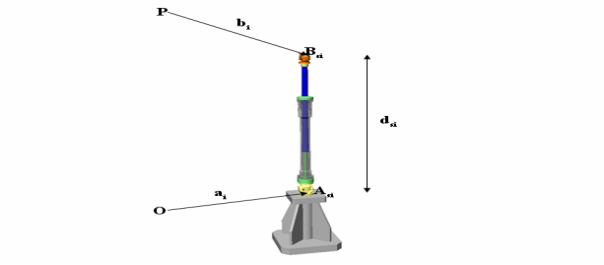

Fig. 3 The straight actuator in the shaking table.

Let d_{si} $i = 1,2,3$ denote the length of the three straight actuators respectively, the following equations represent the inverse kinematics of the straight actuator of the shaking table.

$$d_{si} = \sqrt{[{}^{A}b_i - {}^{A}a_i]^T [{}^{A}b_i - {}^{A}a_i]} \quad i = 1,2,3 \tag{5}$$

In bell crank actuator, points C_{i1} and points C_{i2} are function of θ_i as shown in Fig. 4.

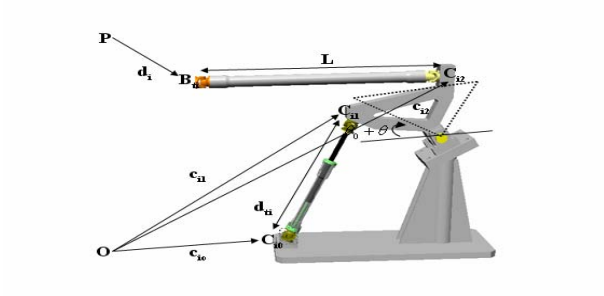

Fig. 4 The bell crank actuator in the shaking table.

Using the constraint condition that the length of crank rod is L, θ_i is computed as

$$L^2 = [{}^{A}c_{i2} - {}^{A}d_i]^T [{}^{A}c_{i2} - {}^{A}d_i] \quad i = 1,2,3. \tag{6}$$

Let d_{ti} $i = 1,2,3$ denote the length of the three bell crank actuators respectively, the following equations represent the inverse kinematics of the bell crank actuator of the shaking table.

$$d_{ti} = \sqrt{[{}^{A}c_{i1} - {}^{A}c_{i0}]^T [{}^{A}c_{i1} - {}^{A}c_{i0}]} \quad i = 1,2,3 \tag{7}$$

2.4 Jacobian

The Jacobian describes the relationship between joint and end-effector velocities. The Jacobian of the shaking table relates velocities of the mass center of the platform to joint velocities as follows

$$\dot{l} = J\dot{x}_p. \tag{8}$$

where l is actuator length vector and x_p is displacement

vector.

In the straight actuator, Jacobian matrix is easily derived applying conventional velocity vector-loop method. Using the definition of angular velocity, the relationship between linear and angular velocity of the platform and the displacement vector can be written as

$$\begin{pmatrix} {}^{A}v_p \\ {}^{A}\omega_p \end{pmatrix} = \begin{pmatrix} 1 & 0 & 0 & 0 & 0 & 0 \\ 0 & 1 & 0 & 0 & 0 & 0 \\ 0 & 0 & 1 & 0 & 0 & 0 \\ 0 & 0 & 0 & u_1\alpha_{s1}+v_1\alpha_{s2} & u_1\beta_{s1}+v_1\beta_{s2}+w_1\beta_{s3} & u_1\gamma_{s1}+v_1\gamma_{s2}+w_1\gamma_{s3} \\ 0 & 0 & 0 & u_2\alpha_{s1}+v_2\alpha_{s2} & u_2\beta_{s1}+v_2\beta_{s2}+w_2\beta_{s3} & u_2\gamma_{s1}+v_2\gamma_{s2}+w_2\gamma_{s3} \\ 0 & 0 & 0 & u_3\alpha_{s1}+v_3\alpha_{s2} & u_3\beta_{s1}+v_3\beta_{s2}+w_3\beta_{s3} & u_3\gamma_{s1}+v_3\gamma_{s2}+w_3\gamma_{s3} \end{pmatrix} \begin{pmatrix} \dot{x} \\ \dot{y} \\ \dot{z} \\ \dot{\alpha} \\ \dot{\beta} \\ \dot{\gamma} \end{pmatrix} = J_m \dot{x}_p \quad (9)$$

where ${}^{A}v_p$ and ${}^{A}\omega_p$ are the linear and angular velocity of the platform respectively and u_i, v_i, w_i, α_{si}, β_{si} and γ_{si} $i=1,2,3$ are the function of α, β and γ. In Fig. 3, the relationship between actuator velocity and ${}^{A}v_p$ and ${}^{A}\omega_p$ can be written as

$$\begin{aligned} {}^{A}a_i + d_{si}\,{}^{A}s_i &= {}^{A}P + {}^{A}b_i \\ &= {}^{A}P + {}^{A}_{B}{}^{B}b_i \\ \dot{d}_{si}\,{}^{A}s_i + d_{si}\cdot{}^{A}\omega^{i} \times {}^{A}s_i &= {}^{A}v_P + {}^{A}\omega_P \times {}^{A}b_i \\ \dot{d}_{si} &= {}^{A}s_i \cdot {}^{A}v_P + ({}^{A}b_i \times {}^{A}s_i)\cdot {}^{A}\omega_P \end{aligned}$$

$$\begin{pmatrix} \dot{d}_{s1} \\ \dot{d}_{s2} \\ \dot{d}_{s3} \end{pmatrix} = \begin{pmatrix} {}^{A}s_1{}^{T} & ({}^{A}b_1 \times {}^{A}s_1)^{T} \\ {}^{A}s_2{}^{T} & ({}^{A}b_2 \times {}^{A}s_2)^{T} \\ {}^{A}s_3{}^{T} & ({}^{A}b_3 \times {}^{A}s_3)^{T} \end{pmatrix} \begin{pmatrix} {}^{A}v_P \\ {}^{A}\omega_P \end{pmatrix}. \quad (10)$$

where ${}^{A}s_i$ is the unit vector from point A_{si} to B_{si}. In Eq. (9) and Eq. (10), Jacobian matrix of the straight actuator can be written as

$$\begin{pmatrix} \dot{d}_{s1} \\ \dot{d}_{s2} \\ \dot{d}_{s3} \end{pmatrix} = \begin{pmatrix} {}^{A}s_1{}^{T} & ({}^{A}b_1 \times {}^{A}s_1)^{T} \\ {}^{A}s_2{}^{T} & ({}^{A}b_2 \times {}^{A}s_2)^{T} \\ {}^{A}s_3{}^{T} & ({}^{A}b_3 \times {}^{A}s_3)^{T} \end{pmatrix} J_m \dot{x}_p = J_s \dot{x}_p. \quad (11)$$

In the bell crank actuator, Jacobain matrix is derived applying velocity vector-loop method and constraint equation. Using vector-loop method as shown in Fig. 4, the following equation is derived as

$$\dot{d}_{ti}\,{}^{A}t_i + d_{ti}\,{}^{A}\dot{t}_i - {}^{A}\dot{c}_{i1} = 0. \quad (12)$$

where ${}^{A}t_i$ is the unit vector from point C_{i0} to C_{i1}. From the constraint condition that the length of crank rod is L, the following equation is derived as

$$L^2 = [{}^{A}d_i - {}^{A}c_{i2}]^{T}[{}^{A}d_i - {}^{A}c_{i2}] \quad i=1,2,3. \quad (13)$$

Since the vector ${}^{A}c_{i2}$ is the function of θ_i, Eq. (13) can be written as

$$\dot{\theta}_i = \frac{1}{R_i}(R_{i1}\dot{x} + R_{i2}\dot{y} + R_{i3}\dot{z} + \alpha_{ti}\dot{\alpha} + \beta_{ti}\dot{\beta} + \gamma_{ti}\dot{\gamma}). \quad (14)$$

where R_i, R_{i1}, R_{i2}, R_{i3}, α_{ti}, β_{ti} and γ_{ti} $i=1,2,3$ are the function of α, β, γ and θ_i. Using the fact that ${}^{A}c_{i1}$ is the function of θ_i, Eq. (12) can be expressed as

$$\dot{d}_{ti} = \frac{1}{t_{i2}}\left[\frac{(c^1_{i2} - c^0_{i2})^2}{d_{ti}^{\,2}} Cp_{i2} + \frac{(c^1_{i2} - c^0_{i2})(c^1_{i3} - c^0_{i3})}{d_{ti}^{\,2}} Cp_{i3}\right]\dot{\theta}_i \quad (15)$$

$${}^{A}t_i = [t_{i1}\ t_{i2}\ t_{i3}]^{T} \quad {}^{A}c_{i0} = [c^0_{i1}\ c^0_{i2}\ c^0_{i3}]^{T} \quad {}^{A}c_{i1} = [c^1_{i1}\ c^1_{i2}\ c^1_{i3}]^{T}.$$

where Cp_{i2} and Cp_{i3} $i=1,2,3.$ are the function of θ_i. Combining Eq. (14) with Eq. (15), the Jacobian matrix of the bell crank actuator can be written as

$$\dot{d}_i = \frac{S_i}{R_i}(R_{i1}\dot{x} + R_{i2}\dot{y} + R_{i3}\dot{z} + \alpha_{ti}\dot{\alpha} + \beta_{ti}\dot{\beta} + \gamma_{ti}\dot{\gamma})$$

$$\begin{pmatrix} \dot{d}_{t1} \\ \dot{d}_{t2} \\ \dot{d}_{t3} \end{pmatrix} = \begin{pmatrix} \frac{S_1}{R_1}R_{11} & \frac{S_1}{R_1}R_{12} & \frac{S_1}{R_1}R_{13} & \frac{S_1}{R_1}\alpha_{t1} & \frac{S_1}{R_1}\beta_{t1} & \frac{S_1}{R_1}\gamma_{t1} \\ \frac{S_2}{R_2}R_{21} & \frac{S_2}{R_2}R_{22} & \frac{S_2}{R_2}R_{23} & \frac{S_2}{R_2}\alpha_{t2} & \frac{S_2}{R_2}\beta_{t2} & \frac{S_2}{R_2}\gamma_{t2} \\ \frac{S_3}{R_3}R_{31} & \frac{S_3}{R_3}R_{32} & \frac{S_3}{R_3}R_{33} & \frac{S_3}{R_3}\alpha_{t3} & \frac{S_3}{R_3}\beta_{t3} & \frac{S_3}{R_3}\gamma_{t3} \end{pmatrix} \dot{x}_P = J_t \dot{x}_P. \quad (16)$$

where S_i is the function of α, β, γ and θ_i. From the Eq. (11) and Eq. (16), the Jacobian matrix of the shaking table can be expressed as

$$\dot{l} = \begin{pmatrix} J_s \\ J_t \end{pmatrix} \dot{x}_P = J \dot{x}_P. \quad (17)$$

2.5 Workspace

In most cases, it is very difficult to exactly calculate the workspace volume of parallel manipulator. The discretization method is efficient and useful. The workspace volume can be numerically approximated by considering a parallelepiped workspace volume V^*, which can be evaluated by considering the extreme reaches, maximum and minimum, along x, y and z axis, if one consider the position space, or the extreme reaches along Euler angles axes, for the orientation workspace.

The factors to determine workspace are maximum stroke of the hydraulic actuator, collision between links and singularity as shown in Fig. 5. Considering maximum stroke and collision, workspace is computed as shown in Table 1.

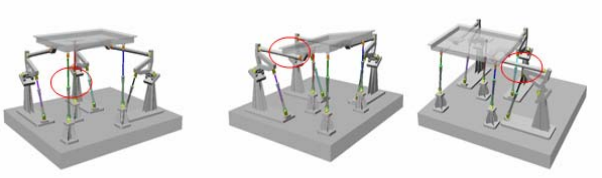

Fig. 5 Maximum stroke and collision between links.

Table 1 The allowable maximum displacement of motion.

Directions	Disp.(mm)	Directions	Disp.(deg)
Longitudinal(x)	-250 ~ +250	Roll(α)	-5 ~ +5
Lateral(y)	-250 ~ +250	Pitch(β)	-5 ~ +5
Heave(z)	-500 ~ +500	Yaw(γ)	-10 ~+10

To check singularity, condition number is introduced. The condition number is defined by Eq. (18)

$$\lambda = \| J \| * \| J^{-1} \| \tag{18}$$

where $\|\cdot\|$ denotes the norm of 2 of a matrix. For high values of λ, there are end-effector directions where the manipulator can develop much higher forces or velocities than in other directions. In many applications, this is not a desirable system property. The condition number is plotted for the position workspace at $z = 200mm$ and for the orientation workspace at $\gamma = 3^{\circ}$ as shown in Fig. 6.

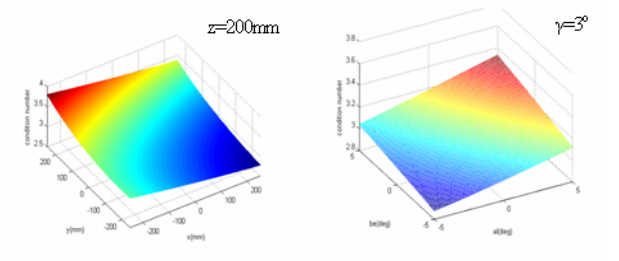

Fig. 6 Condition number
for the position and orientation workspace.

Fig. 6 shows the workspace is well conditioned and the system is away from singular conditions.

3. DYNAMICS

To derive parallel algorithms, each of the unknown forces and torques associated with one particular leg is decomposed into one vector in the direction of the leg and the other vector acting in a plane orthogonal to the leg.

In straight actuator, the free body diagram of the upper and lower part of the leg is represented in Fig. 7.

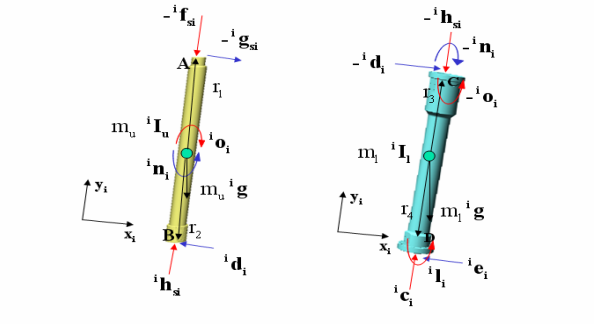

Fig. 7 Free body diagram of the upper and lower part
of the straight actuator.

From Fig. 7 the equations are obtained as follows: first, the upper part is considered. The forces and moments are summed in the plane orthogonal to the direction of the leg, which leads to

$$\begin{aligned} &{}^{i}d_i - {}^{i}g_{si} + m_u\, {}^{i}g^{\perp} = m_u\, {}^{i}a_{ui}^{\perp} \\ &{}^{i}r_1 \times {}^{i}d_i - {}^{i}r_2 \times {}^{i}g_{si} + {}^{i}n_i = {}^{i}I_u\, {}^{i}\dot{\omega}_i + {}^{i}\omega_i \times {}^{i}I_u\, {}^{i}\omega_i . \end{aligned} \tag{19}$$

where i frame is attached to the actuator and ${}^{i}a_{ui}^{\perp}$ is the acceleration of the center of mass of the upper part in the plane orthogonal to the direction of the upper part. The same equations are applied to the lower part. This leads to

$$\begin{aligned} &-{}^{i}d_i + {}^{i}e_i + m_l\, {}^{i}g^{\perp} = m_l\, {}^{i}a_{li}^{\perp} \\ &-{}^{i}r_3 \times {}^{i}d_i + {}^{i}r_4 \times {}^{i}e_i - {}^{i}n_i = {}^{i}I_l\, {}^{i}\dot{\omega}_i + {}^{i}\omega_i \times {}^{i}I_l\, {}^{i}\omega_i . \end{aligned} \tag{20}$$

where ${}^{i}a_{li}^{\perp}$ is the acceleration of the center of mass of the lower part in the plane orthogonal to the direction of the lower part. These last two vectors are obtained from the kinematic analysis. From Eq. (19) and Eq. (20), this system forms 8 scalar equations in 8 unknowns, the unknowns being the components of ${}^{i}d_i, {}^{i}g_{si}, {}^{i}n_i$ and ${}^{i}e_i$. The solution of this system will lead to the determination of the components of vector ${}^{i}g_{si}$.

In bell crank actuator, since the crank rod is connected to the platform, the free body diagram of the crank rod is represented in Fig. 8 to determine the orthogonal component.

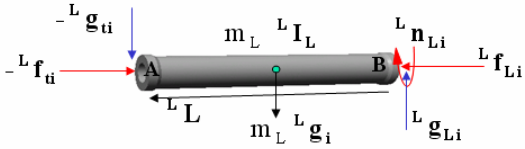

Fig. 8 Free body diagram of the crank rod
of the bell crank actuator.

Applying the Euler equation, the following equation is derived as

$${}^{L}L \times (-{}^{L}g_{ti}) + \frac{{}^{L}L}{2} \times m_L\, {}^{L}g_i = {}^{L}I^{B}_{L}\, {}^{L}\dot{\omega}_{Li} + {}^{L}\omega_{Li} \times {}^{L}I^{B}_{L}\, {}^{L}\omega_{Li} . \tag{21}$$

where L frame is attached to the crank rod and ${}^{L}I^{B}_{L}$ is the inertia tensor for point B. The orthogonal vector ${}^{L}g_{ti}$ can be determined from the Eq. (21).

When the determination of the orthogonal components is performed for each leg - in parallel –, only 6 unknown quantities will remain on the free body diagram of the platform, i.e., the forces in the direction of each leg. Applying Newton-Euler equation to the platform, the following equations are obtained as

$$\begin{aligned} &{}^{A}F + {}^{A}G + m_p\, {}^{A}g = m_p\, {}^{A}\dot{v}_p \\ &{}^{B}n_p = \sum_{i=1}^{3} {}^{B}b_i \times {}^{B}f_{si} + \sum_{i=1}^{3} {}^{B}b_i \times {}^{B}g_{si} + \sum_{i=1}^{3} {}^{B}d_i \times {}^{B}f_{ti} + \sum_{i=1}^{3} {}^{B}d_i \times {}^{B}g_{ti} \end{aligned} \tag{22}$$

with

$$F_s=\sum_{i=1}^{3}{}^{A}f_{si}\quad F_t=\sum_{i=1}^{3}{}^{A}f_{ti}\quad F=F_s+F_t$$
$$G_s=\sum_{i=1}^{3}{}^{A}g_{si}\quad G_t=\sum_{i=1}^{3}{}^{A}g_{ti}\quad G=G_s+G_t.$$

where ${}^{B}n_p$ is the sum of the moments applied to the platform.

Using the solution of Eq. (22), the hydraulic actuator force ${}^{i}h_{si}$ in the straight actuator can be obtained applying to Newton equation to each of the upper parts of the legs, in the direction of the leg. This leads to

$$-{}^{i}f_{si}+{}^{i}h_{si}+m_u{}^{i}g_i^{\parallel}=m_u{}^{i}a_{ui}^{\parallel}. \tag{23}$$

where ${}^{i}a_{ui}^{\parallel}$ is the acceleration in the direction of the leg.

Since the upper and lower part of the bell crank actuators are not directly connected to the platform, the hydraulic actuator force ${}^{i}h_{ti}$ can be obtained after the dynamics of the crank and crank rod is analyzed. From Fig. 8, using the orthogonal component ${}^{L}g_{ti}$ and directional component ${}^{L}f_{ti}$, the ${}^{L}g_{Li}$ and ${}^{L}f_{Li}$ can be obtained from the following equation as

$$\begin{aligned}&-{}^{L}g_{ti}+{}^{L}g_{Li}+m_L{}^{L}g_i^{\perp}=m_L{}^{L}a_{Li}^{\perp}\\&-{}^{L}f_{ti}+{}^{L}f_{Li}+m_L{}^{L}g_i^{\parallel}=m_L{}^{L}a_{Li}^{\parallel}.\end{aligned} \tag{24}$$

where ${}^{L}a_{Li}^{\perp}$ and ${}^{L}a_{Li}^{\parallel}$ are the orthogonal and directional acceleration of the crank rod respectively.

To obtain the directional component of the upper part in the bell crank actuator, orthogonal component ${}^{i}g_{Ai}$ must be determined. The free body diagram of the upper and lower part of the bell crank actuator is represented in Fig. 9. Unlike the straight actuator, the upper and lower part of the bell crank actuator move on the plane. The forces and moments are summed in the plane orthogonal to the direction of the leg, which leads to

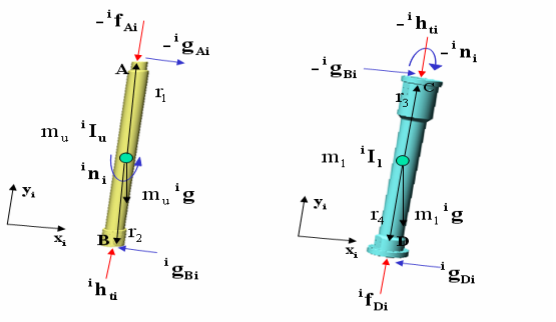

Fig. 9 Free body diagram of the upper and lower part of the bell crank actuator.

$$\begin{aligned}&(r_2+r_1)y_i\times(-{}^{i}g_{Ai})+{}^{i}n_i+r_2y_i\times m_u{}^{i}g={}^{i}I_u^{B}{}^{i}\dot{\omega}_i\\&(r_1+r_2)y_i\times{}^{i}g_{Bi}+{}^{i}n_i+r_1y_i\times m_u{}^{i}g={}^{i}I_u^{A}{}^{i}\dot{\omega}_i\\&(r_4+r_3)y_i\times(-{}^{i}g_{Bi})-{}^{i}n_i+r_4y_i\times m_l{}^{i}g={}^{i}I_l^{D}{}^{i}\dot{\omega}_i.\end{aligned} \tag{25}$$

From Eq. (25), this system forms 3 scalar equations in 3 unknowns, the unknowns being the components of ${}^{i}g_{Ai}, {}^{i}g_{Bi}$ and ${}^{i}n_i$. The solution of this system will lead to the determination of the component ${}^{i}g_{Ai}$.

Using transformation between two frames, the force ${}^{A}f_{Ai}$ acting in the crank can be expressed as the function of ${}^{i}f_{Ai}$.

$${}^{A}f_{Ai}={}_{i}^{A}R\,{}^{i}g_{Ai}+{}_{i}^{A}R\,{}^{i}f_{Ai}={}_{i}^{A}R\,{}^{i}g_{Ai}+\begin{pmatrix}g_1({}^{i}f_{Ai})\\g_2({}^{i}f_{Ai})\end{pmatrix} \tag{26}$$

Finally, the dynamics of the crank is analyzed to determine the directional component ${}^{i}f_{Ai}$. The free body diagram of the crank is represented in Fig. 10.

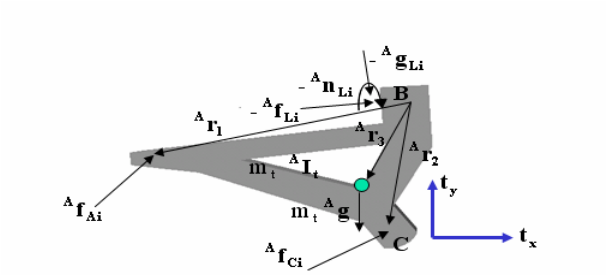

Fig. 10 Free body diagram of the crank.

Applying the Newton-Euler equations, the following equations are derived as

$$\begin{aligned}&{}^{A}f_{Ai}+{}^{A}f_{Ci}-{}^{A}f_{Li}-{}^{A}g_{Li}+m_t{}^{A}g=m_t{}^{A}a_{ti}\\&{}^{A}r_1\times{}^{A}f_{Ai}+{}^{A}r_2\times{}^{A}f_{Ci}+{}^{A}r_3\times m_t{}^{A}g={}^{A}I_t^{B}{}^{A}\dot{\omega}_{ti}.\end{aligned} \tag{27}$$

where ${}^{A}a_{ti}$ is acceleration of the crank. From Eq. (27), the directional component ${}^{i}f_{Ai}$ can be obtained.

The hydraulic actuator force ${}^{i}h_{ti}$ in the bell crank actuator can be obtained applying to the Newton equations to each of the upper parts of the legs. This leads to

$$-{}^{i}f_{Ai}+{}^{i}h_{ti}+m_u{}^{i}g_i^{\parallel}=m_u{}^{i}a_{ui}^{\parallel}. \tag{28}$$

The solution of inverse dynamics derived above is almost completely parallel. Only one of the steps - the application of the Newton-Euler equations to the platform – must be performed on one single processor.

4. CONTROL

For the tracking control of manipulators, joint-based control schemes have been used. The joint-based control schemes, that is, schemes in which we develop trajectory errors by finding the difference between desired and actual quantities expressed in joint space. An alternative approach is Cartesian-based control which is based on forming errors in Cartesian space.

In the tracking control of parallel manipulators, model based control schemes such as computed torque method and

sliding mode control were proposed. Since these control schemes use joint based reference input and measured output, synchronous problem can occur. Cartesian-based scheme can be more efficient than joint-based scheme if synchronousness is considered. However, Cartesian-based controllers must perform many computations in the loop because of the kinematics and other transformations which are inside the loop.

Joint-based control using Cartesian-based command generator is proposed as shown in Fig. 11.

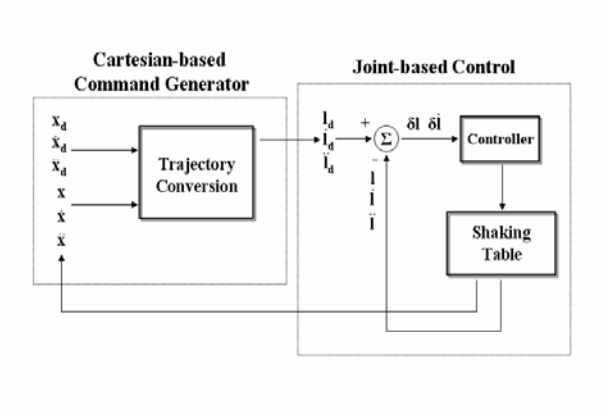

Fig. 11 Joint-based control
using Cartesian-based command generator.

Unlike the previous joint-based control schemes, this control scheme uses sensors attached to the platform as well as sensors attached to the actuators. Consequently, there is no need for solving the forward kinematic problem with highly nonlinear simultaneous equations. Using trajectory conversion, the joint-based control is performed.

5. CONCLUSION

In this paper, 6-DOF shaking table with a bell crank structure was introduced. The bell crank mechanism is used to reduce the amount of space needed to install and create horizontal motion. In kinematics, joint design was performed using Grübler's formula. The Jacobian matrix was derived in the velocity domain and used to check singularities. Considering the maximum stroke, collision and singularity, workspace was computed.

In dynamics, the solution of inverse dynamics was obtained using the Newton-Euler method. To derive parallel algorithms, each contact force was decomposed into one force acting in the direction of the leg and the other acting in the plane orthogonal to the direction of the leg. Except for the application of the Newton-Euler equations to the platform, processors were completely parallel.

Considering synchronous problem, we proposed the joint-based control using Cartesian-based command generator for the tracking control of the shaking table. Unlike the previous control schemes, Cartesian information is directly measured. Using joint-based control schemes such as computed torque method and sliding mode control, the proposed control algorithm will be verified. This is left for the future work.

ACKNOWLEDGMENTS

This work was supported by the Brain Korea 21, the National Research Laboratory and the Korea Institute of Machinery and Materials, Daejeon, Korea.

REFERENCES

[1] J. C. Shin, "Robust control of motion system and estimation of rider's action force for bicycle simulator," *Ph.D Thesis, KAIST*, 2003.

[2] C. Gosselin, "Parallel computational algorithms for the kinematics and dynamics of parallel manipulators," *Proc. of the IEEE Conf. on Robotics and Automation*, Vol. 1, pp. 883-888, 1993..

[3] W. J. Chen, M. Y. Zhao and S. H. Chen, "A novel 4-DOF parallel manipulator and its kinematic modeling," *Proc. of the IEEE Conf. on Robotics and Automation*, Vol. 4, pp. 3350-3355, 2001.

[4] K. Cleary and M. Uebel, "Jacobian formulation for a novel 6-DOF parallel manipulator," *Proc. of the IEEE Conf. on Robotics and Automation*, Vol. 3, pp. 2377-2382, 1994.

[5] R. E. Stamper, L. W. Tsai and G. C. Walsh, "Optimization of a three DOF translational platform for well-conditioned workspace," *Proc. of the IEEE Conf. on Robotics and Automation*, Vol. 4, pp. 3250-3255, 1997.

[6] J. J. Craig, *Introduction to Robotics Mechanics and Control*, Addison-Wesley Publishing Company, 1986.

[7] J. A. Carretero, M. Nahon and R. P. Podhorodeski, **"**Workspace analysis of a 3-DOF parallel mechanism," *Proc. of the IEEE Conf. on Intelligent Robots and Systems*, Vol. 2, pp. 1021-1026, 1998.

[8] E. Ottaviano and M. Ceccarelli, "Optimum design of parallel manipulators for workspace and singularity performances," *Proc. of the Workshop on Fundamental Issues and Future Research Directions for Parallel Mechanisms and Manipulators*, pp.98-105, 2002.